Supplementary File for

The 2024 cascading glacial lake outburst flood in the Thame Valley of Everest region, Nepal: process, impacts and implications

Nitesh Khadka[1], Vishnu Prasad Pandey[1, 2 *], C. Scott Watson[3], Guoxiong Zheng[4, 5], Tianpei Wu[6,7], Keshab Sharma[8], Lauren D. Rawlins[3], Simon Allen[9], Manish Raj Gouli[10], Dibas Shrestha[11]

[1]Center for Water Resources Studies (CWRS), Institute of Engineering, Tribhuvan University, Lalitpur, Nepal

[2]Department of Civil Engineering, Pulchowk Campus, Institute of Engineering, Tribhuvan University, Lalitpur, Nepal

[3]School of Geography and water@leeds, University of Leeds, Leeds, UK

[4]College of Earth and Environmental Sciences, Lanzhou University, Lanzhou, China

[5]Midui Glacier-Guangxie Lake Disaster Field Science Observation and Research Station of Tibet Autonomous Region, Northwest Institute of Eco-Environment and Resources, Chinese Academy of Sciences, Lanzhou, China

[6]State Key Laboratory of Mountain Hazards and Engineering Resilience, Institute of Mountain Hazards and Environment, Chinese Academy of Sciences, Chengdu, China

[7]University of Chinese Academy of Sciences, Beijing, China

[8]BGC Engineering Inc., 330 AlisonBlvd., Fredericton, NB, Canada E3C 0A9

[9]Department of Geography, University of Zurich, Zurich, Switzerland

[10]The Stimson Center - Energy, Water, & Sustainability, 1211 Connecticut Ave, NW / 8th Floor Washington, DC 20036

[11]Central Department of Meteorology and Hydrology, Tribhuvan University, Kathmandu, Nepal

***Correspondence:** Vishnu Prasad Pandey (vishnu.pandey@pcampus.edu.np)

Text S1. Pre- and post-GLOF lake outlines were used to derive the lower lake volumes. These volumes were calculated by integrating the bathymetric survey conducted in May 2025 with a 1 m resolution drone-derived digital elevation model (DEM) from the same period. For each time interval, lake outlines were used to determine a mean water level elevation and its associated standard deviation (SD). Volumes were then computed based on the depth of all lake cells relative to the mean lake elevation. To quantify uncertainty, this process was repeated using the mean elevation ± SD, with the maximum spread in the derived volume taken as the uncertainty estimate. The standard deviations were 2.6 m for the pre-GLOF outline and 2.5 m for the post-GLOF outline. These results indicate that even a few meters of variation in lake level can substantially influence the estimated volume.

The lake volume and drainage volume values (Table below) obtained from field are quite similar to the values obtained from empirical analysis (Table S1).

Table The lake volume derived from field data.

Date	**Lake volume (m^3)**	**Uncertainty (m^3)**
Pre-GLOF 30-May-24	462,281	136,411
Post-GLOF 18-Aug-24	98,741	50,718
Drained Volume	363,540 m^3 (351,171 m^3 from empirical estimations)	

Text S2 The accuracy assessment of GLOF reconstruction was conducted by comparing the satellite-derived inundation area with the modeled flood extent. True Positive (TP) are the areas flooded in both satellite and model, whereas False Negative (FN) are areas flooded in satellite but not in model (underprediction) and False Positive (FP) are areas flooded in model but not in satellite (overprediction). **Precision** quantifies the reliability of the model's flood predictions, representing the proportion of predicted flooded areas that were actually flooded. **Recall** measures the model's completeness, representing the proportion of actual flooded areas that were correctly captured by the model. **F1 Score** provides a single metric that balances precision and recall by computing their harmonic mean. This is particularly useful when evaluating models where both overprediction and underprediction have important implications, as is the case for GLOF hazard assessment

$$\boldsymbol{Precision} = \frac{TP}{TP + FP}$$

$$\boldsymbol{Recall} = \frac{TP}{TP + FN}$$

$$\boldsymbol{F1\ Score} = 2 \times \frac{Precision \times Recall}{Precision + Recall}$$

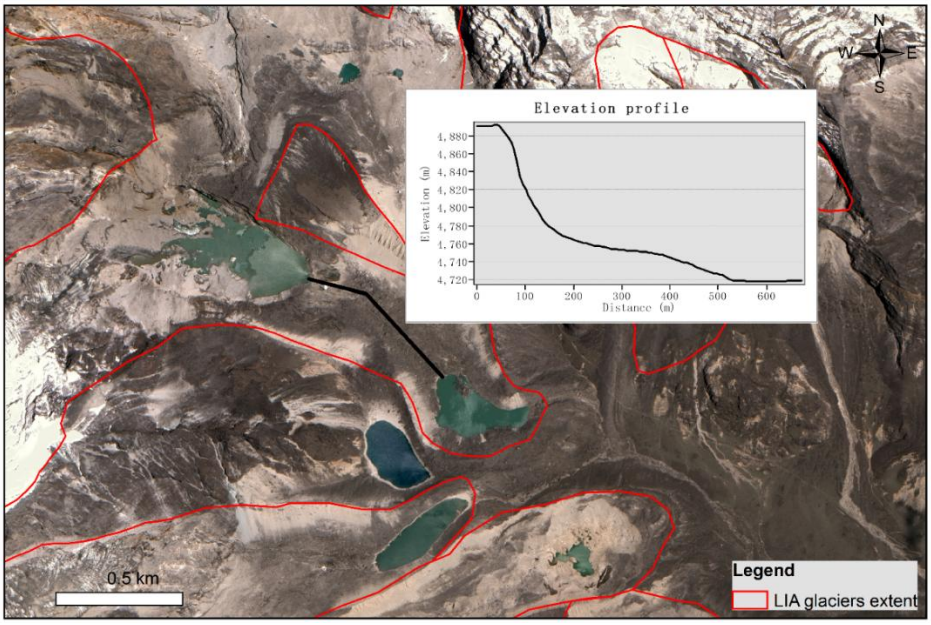

Figure S1 *Elevation profile of flow path connectivity (channel) between upper and lower glacial lakes derived from HMA-DEM along with Little Ice Age (LIA) glacier extent. The LIA glacier outlines were obtained from Lee et al. (2021). The background is from Gaofen image of 2024-5-30. The figure was created by authors using ArcGIS® software by Esri.*

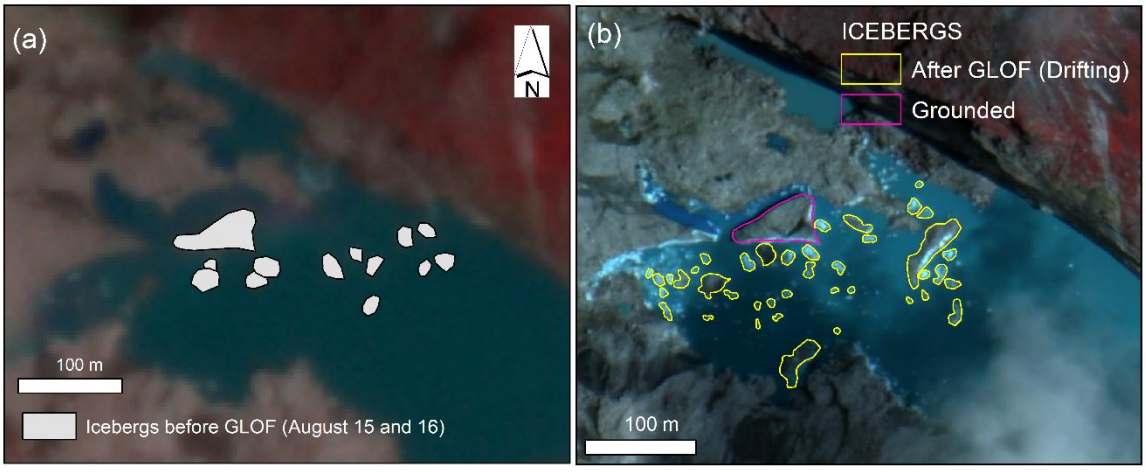

Figure S2 *The ice-bergs delineated before the GLOF event from Planetscope images of 2024 August 15 and 16 (a) and from Gaofen image of 2024-8-18 after its outburst (b). The figure was created by authors using ArcGIS® software by Esri.*

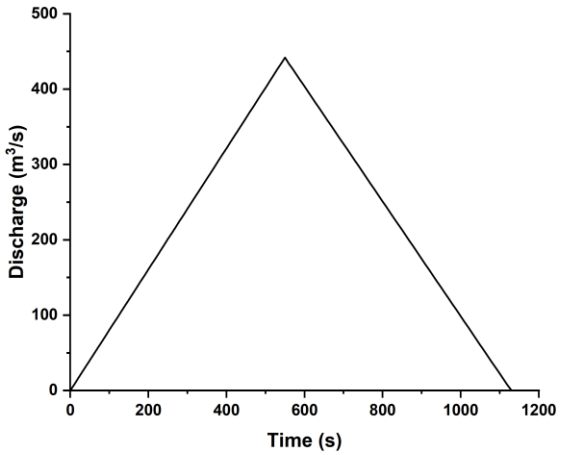

Figure S3 *Inflow discharge at upstream input 1 for Scenario A.*

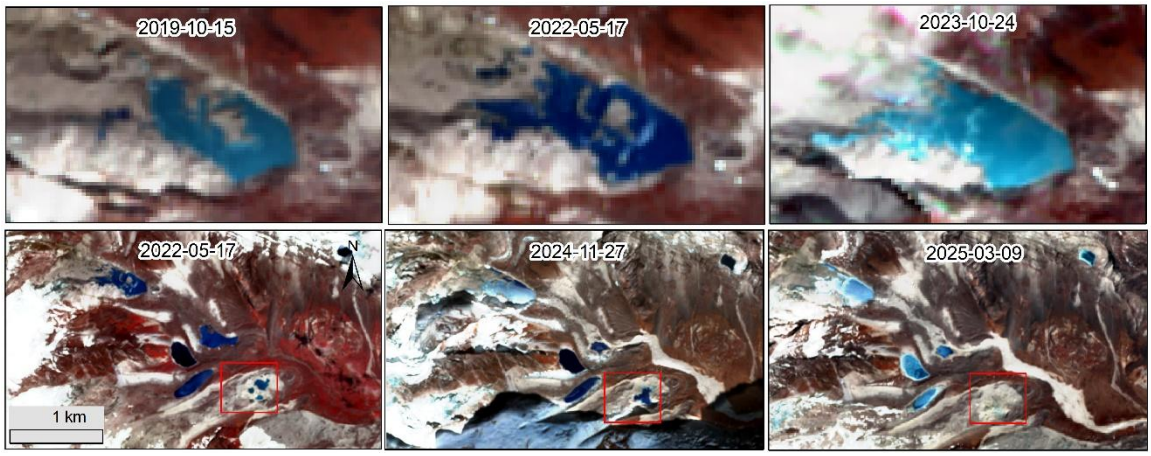

Figure S4 *The rapid expansion of upper lake between 2019 and 2023 (upper panel) and ephemeral nature of lake 5 (red box) shown by Sentinel timeseries images. The figure was created by authors using ArcGIS® software by Esri.*

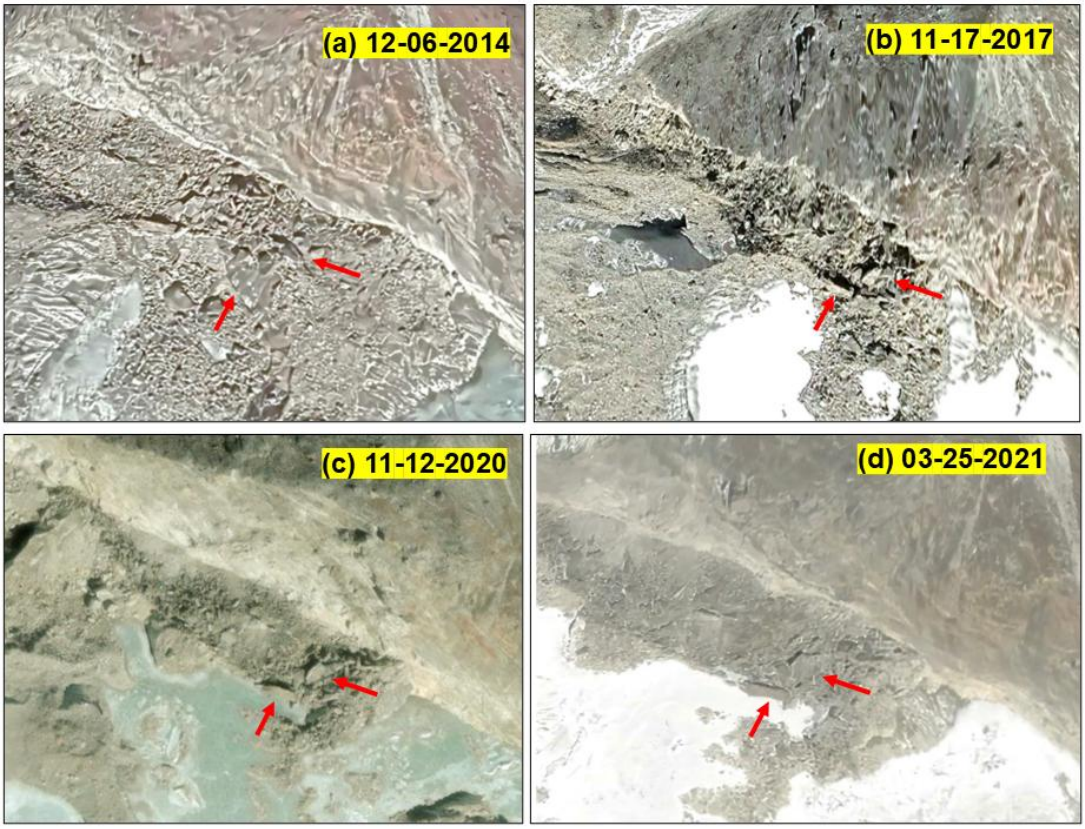

Figure S5 *The time series satellite images showing the deposition of rockfalls pre-GLOF from 2014 to 2021. The images in a, b and d are from © Google Earth collection; images: © CNES/Airbus, Maxar Technologies, Airbus CNES/Airbus and c is from ESRI (Sources: Esri, TomTom, FAO, USGS | Powered by Esri).*

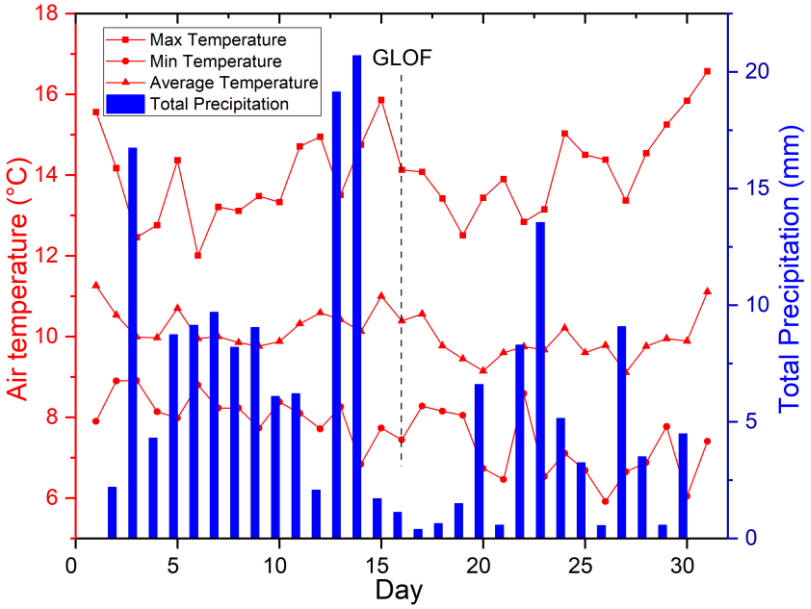

Figure S6 *The climatology of August month obtained from Phortse Automatic Weather Station.*

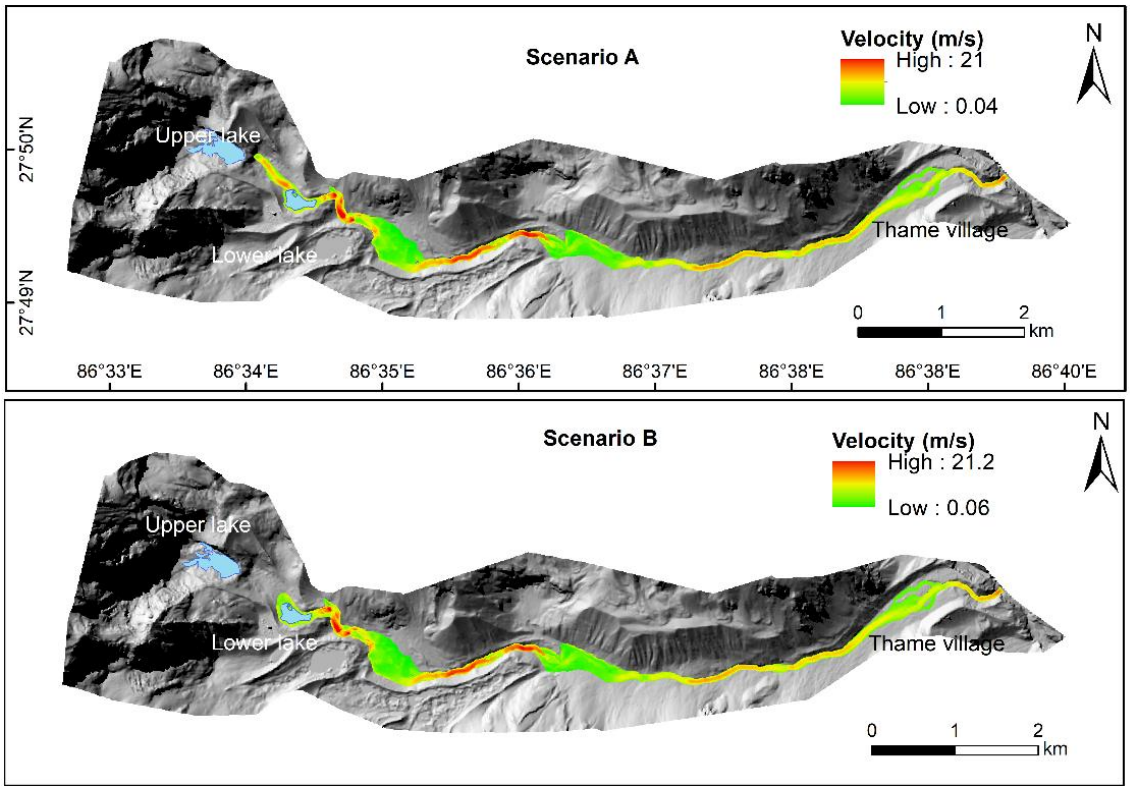

Figure S7 *Simulation results of velocity maps for scenarios A and B. The background is hill shade of HMA DEM. The figure was created by authors using ArcGIS® software by Esri.*

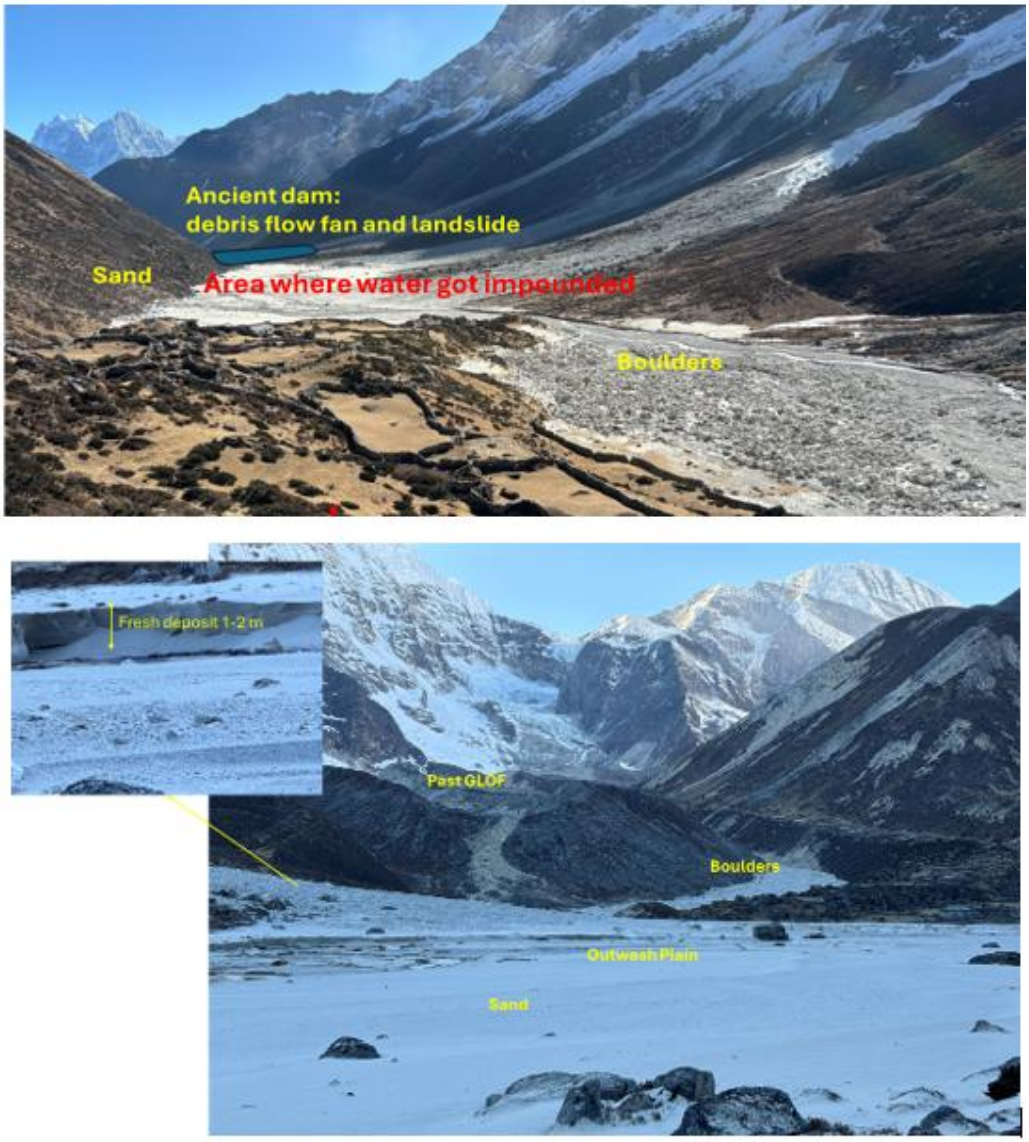

Figure S8 *The ancient debris flow and landslide dam downstream of Thengpo Village where GLOF water got impounded for temporary field. Photo by K. Sharma, 2024.*

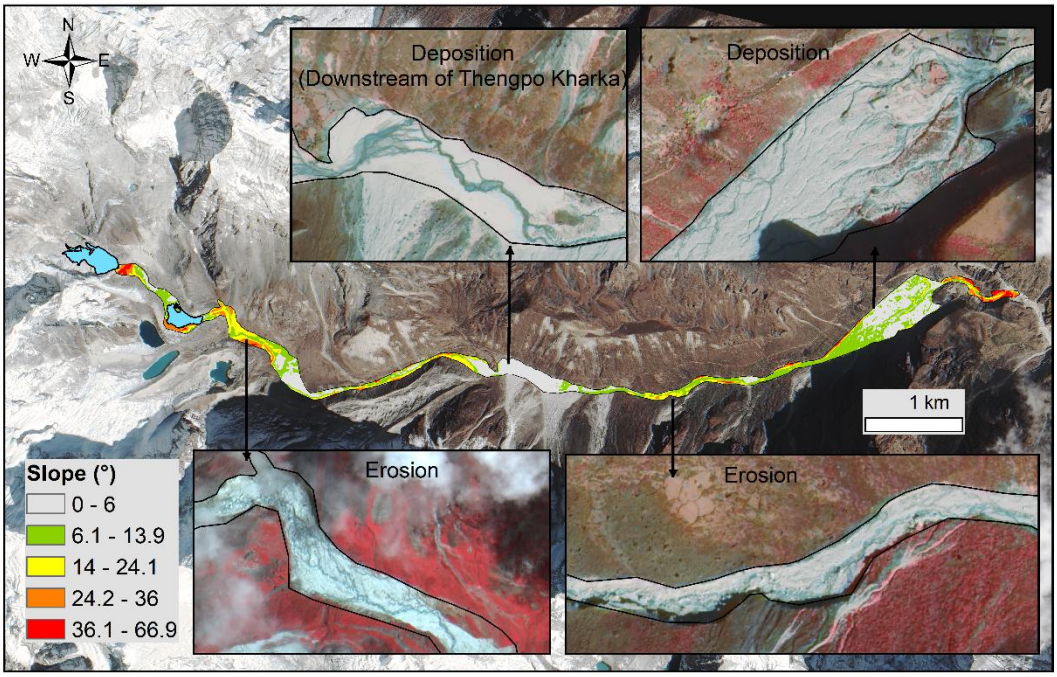

Figure S9 *The erosion and deposition zones along the river channel due to GLOF event. The base map is from Gaofen image of August 18, 2024. The figure was created by authors using ArcGIS® software by Esri.*

Figure S10 *Ongoing channel erosion and debris deposition along the Thame stream in Thame Valley, Nepal, showing the close interaction between active geomorphic processes and nearby settlements and infrastructure. Photo by N. Khadka, 2024.*

Table S1 *The volume of glacial lakes before and after their outburst estimated from empirical equations. The lake area and volume are in m^2 and m^3 unless otherwise stated.*

Equation	**Description**	**Volume before outburst**		**Volume after outburst**		**Difference**		Reference
		Upper lake	**Lower lake**	**Upper lake**	**Lower lake**	**Upper**	**Lower**	
$V=0.035A^{1.5}$	A= lake area	1276900.54	368069.56	1057366.74	70835.02	219533.80	297234.54	Evans (1986)
$V=0.104A^{1.42}$	A= lake area	1499032.17	461738.3	1253860.44	97025.01	245171.73	364713.29	Huggel et al. (2002)
$V=A\cdot D$, where $D=0.087A^{0.434}$	A= lake area; D=depth (m)	1475286.48	449178.74	1231827.57	92945.27	243458.91	356233.47	Wang et al. (2012)
$V=43.24A^{1.5307}$	A in km^2 and V in 10^6 m^3	1474299	414287.5	1216122.6	77085.43	258176.40	337202.07	Sakai (2012)
$V=0.0578A^{1.4683}$	A= lake area	1459502.08	431911.09	1213402.19	86067.11	246099.89	345843.98	Khanal et al. (2015)
$V=0.1217A^{1.4129}$	revised fit of Huggel et al. (2002)	1615378.52	500514.11	1352385	105996.5	262993.52	394517.61	Cook and Quincey (2015)
$V=0.036A^{1.49}$	A= lake area	1169439.08	339900.62	969599.5	66136.51	199839.58	273764.11	Kapitsa et al. (2017)
$V=42.95A^{1.408}$	A in km^2 and V in 10^6 m^3	1919747.3	597242.68	1608191.5	1608191.5	311555.80	470078.68	Zhang et al. (2023a)
$V=48.58A^{1.59}$	For periglacial lake (lower lake)		388714.81		67765.44		320949.37	Zhang et al. (2023b)
$V=44.47A^{1.5}$	For proglacial lake (upper lake)	1622393.35		1343459.97		278933.38		
Average		1501330.95	439061.9	1249579.50	87891.14	251751.44	351170.8	
Volume released (m^2)						**~$2.5*10^5$**	**~$3.5*10^5$**	

Table S2 *Estimation of peak discharge and breach time from different empirical equations. The Q_p, V_G, B_d and T_b are in m^3/s, m^3, m and seconds, unless otherwise stated. Here, breach depth (B_d) is lake level change after GLOF, which is 4.6 and 12 m for upper and lower lake, respectively and for cascading the lower lake breach depth is considered.*

Equation	Description	Upper lake	Lower lake	Upper+lower released volume (cascading)	Source
Peak discharge (Q_p)					
$Q_p=0.72V_G^{0.53}$	V_G= volume released	522.69	624.73	831.3	Evans (1986)
$Qp=0.0048V_G^{0.896}$	V_G= volume released	329.46	445.38	721.88	Popov (1991)
$Q_p = 136\cdot(B_d\cdot V_G)^{0.73}$	V_G= volume released in Mm^3 B_d= breach depth (lake level change)	150.68	387.72	567.63	COSTA and SCHUSTER (1988)
$Q_p=1.122V_G^{0.57}$	V_G= volume	1339.12	1622.23	2205.67	Costa (1985)
$Q_p=0.981(V_G\cdot B_d)^{0.42}$	V_G= volume	344.47	593.52	744.31	Costa (1985)
$Q_p= 0.607(B_d^{1.24}\cdot V_G^{0.295})$	V_G= volume B_d= breach depth	157.54	571.32	669.78	Froehlich (1995)
$Q_p=142\cdot B_d^{0.766}\cdot V_G^{0.378}$	V_G= volume released in Mm^3 B_d= breach depth	270.63	640.62	780.42	Froehlich (2025)
Average		**444.93**	**697.93**	**899.22**	
Breach Time (T_b)					
$T_b=0.00254(V_G)^{0.53}\cdot B_d^{-0.9}$	V_G= volume released B_d= breach depth	1680.98	847.68	1127.96	Froehlich (1995)
$T_b= [V_G^{0.622}/(71\cdot B_d^{0.766})] \cdot 10^6$	V_G= volume released in Mm^3 B_d= breach depth	1847.51	1092.7	1527.92	Froehlich (2025)
Average		**1764.25**	**970.19**	**1327.94**	

Table S3 *The areas of Lakes 3, 4 and 5 in different time delineated from Sentinel-2 images.*

Date	Lake No	Area (km^2)	Error (km^2)	Perimeter (km)
1976-11-13	3	0.052	0.026	0.88
1989-11-09	3	0.055	0.014	0.96
1995-10-09	3	0.055	0.014	0.91
2000-11-23	3	0.057	0.014	0.93
2005-11-10	3	0.056	0.014	0.93
2009-10-05	3	0.057	0.014	0.93
2015-11-17	3	0.057	0.014	0.93
2020-10-09	3	0.053	0.004	0.90
2024-5-30	3	0.042	0.001	0.81
1976-11-13	4	0.063	0.030	0.98
1989-11-09	4	0.067	0.016	1.08
1995-10-09	4	0.073	0.017	1.12
2000-11-23	4	0.068	0.016	1.10
2005-11-10	4	0.068	0.017	1.11
2009-10-05	4	0.066	0.016	1.10
2015-11-17	4	0.067	0.016	1.08
2020-10-09	4	0.055	0.005	1.06
2024-5-30	4	0.042	0.001	0.99
2020-10-09	5	0.048	0.005	0.93
2024-05-17	5	0.021	0.005	0.93
2024-11-27	5	0.027	0.004	0.83
2024-5-30	5	0.011	0.001	0.70
2025-9-3	5	0.006	0.001	0.40

Table S4 *GLOF susceptibility assessment of upper and lower lakes (GAPHAZ 2017). An expert assessment of high (∗∗∗), moderate (∗∗), and low (∗) susceptibility for each of the factors is indicated. Factors not considered relevant for these lakes are indicated with –.*

Susceptibility factors for GLOFs	**Relevance**			**Key Attributes**	**Susceptibility of each lake**		**Assessment methods and/or data**
	Con.	**Trig.**	**Mag.**		**Upper lake**	**Lower lake**	
1. Atmospheric factor							
Temperature	+	+		Mean temperature	*Increasing* ***	*Increasing* ***	ERA5-Land data analysis
	+	+		Intensity and frequency of extreme temperature	*Evident* ***	*Evident* ***	
Precipitation		+	+	Intensity and frequency of extreme precipitation	*Evident* ***	*Evident* ***	
2. Cryospheric factor							
Permafrost conditions	+	+	+	State of permafrost, distribution and persistence within lake dam area and bedrock surrounding slopes	*The presence of permafrost in the dam and the surrounding slope is not evident and is located above 5000 m* *	*The presence of permafrost in the dam and the surrounding slope is not evident* -	Google Earth imagery and (Singh et al. 2025)
Glacier retreat and down wasting	+		+	Enlargement of proglacial lakes, enhanced supraglacial lake formation, dam removal or subsidence.	*Glaciers in the catchment are shrinking and lake has capacity to expand upwards due to glacier calving* ***	*No capacity to expand* *	Ice thickness data and this study
Ice avalanche potential		+	+	Steep glacier tongue or ice cliffs, crevasse density and orientation, ice geometry	*Has potential ice avalanche area from the western northern zone* ***	*None* -	This study and trajectory study
Advancing glacier (incl. su rging)	+			Formation of ice-dammed lakes	*Not relevant* -	*Not relevant* -	Google Earth
Glacier flow regime	+			Glacier flow velocity	*Relevant* *	*Not relevant: no glacier* -	(Gardner et al., 2019)
Calving potential		+	+	Width of glacier calving front, activity, crevasse density	*Wide Calving front and actively calving* ***	*Glacier not in contact with lake* -	This study
Lake size	+		+	Area, volume, and/or depth	*Volume: 1249579.50 m^3* **	*Volume: 87891.14 m^3* *	This study
3. Geotechnical and geomorphic							
Dam type	+		+	Bedrock, moraine, ice	*Bed rock* *	*Moraine* **	Field study
Ice cored moraine	+			Presence of buried ice	*No* -	*No* -	Field study

Downstream slope of dam	+			Steep Lakefront Area angle greater than 10º	*Yes* *	*No* -	Google Earth
Vegetation on dam	+			Density and type of vegetation (grass, shrubs, trees)	*None* -	*None* -	Field photo and Google Earth imagery
Catchment area	+			Total size of drainage area upstream of catchment	*5 km^2* *	*9 km^2* **	DEM and GIS-based modelling
Catchment drainage density	+			Density of the stream network in the catchment area	*Higher than lower lake* *	*Low* *	DEM, GIS-based modelling
Catchment stream order	+			Presence of large fluvial stream facilitating rapid drainage into lake	*Medium order* *	*High order* *	DEM, GIS-based modelling
Upstream lake		+	+	Presence and susceptibility of upstream lakes	*No lakes* -	*One lake* ***	Satellite image
Rock avalanche potential		+	+	Steep, structurally unstable bedrock slopes with potential to runout into the lakes	*Has a large topographic potential of rockfall or rockslides* ***	*None* -	DEM, GIS-based modelling
Side moraine instabilities		+	+	Potential for landslides from moraine slopes into the lake	*Insignificant as lateral moraine is made up of bedrock* -	*Have possibilities but the gradient is low* *	Field and Google Earth
Seismicity		+		Peak ground acceleration	*High* ***	*High* ***	PGA Seismic maps (Rahman and Bai 2018)

References:

Cook, S., & Quincey, D. (2015). Estimating the volume of Alpine glacial lakes. *Earth Surface Dynamics, 3*, 559

Costa, J.E. (1985). *Floods from dam failures*. US Geological Survey

COSTA, J.E., & SCHUSTER, R.L. (1988). The formation and failure of natural dams. *GSA Bulletin, 100*, 1054-1068

Evans, S.G. (1986). The maximum discharge of outburst floods caused by the breaching of man-made and natural dams. *Canadian Geotechnical Journal, 23*, 385-387

Froehlich, D. (2025). Predicting Peak Discharge of Outburst Floods from Moraine-Dammed Glacial Lakes. *Natural Hazards Review, 26*, 04025047

Froehlich, D.C. (1995). Peak outflow from breached embankment dam. *Journal of water Resources Planning and management, 121*, 90-97

GAPHAZ (2017). Assessment of Glacier and Permafrost Hazards in Mountain Regions – Technical Guidance Document. . In S. Prepared by Allen, Frey, H., Huggel, C. et al. Standing Group on Glacier and Permafrost Hazards in Mountains (GAPHAZ) of the International Association of Cryospheric Sciences (IACS) and the International Permafrost Association (IPA). (Ed.) (p. 72). Zurich, Switzerland / Lima, Peru,

Huggel, C., Kääb, A., Haeberli, W., Teysseire, P., & Paul, F. (2002). Remote sensing based assessment of hazards from glacier lake outbursts: a case study in the Swiss Alps. *Canadian Geotechnical Journal, 39*, 316-330

Kapitsa, V., Shahgedanova, M., Machguth, H., Severskiy, I., & Medeu, A. (2017). Assessment of evolution and risks of glacier lake outbursts in the Djungarskiy Alatau, Central Asia, using Landsat imagery and glacier bed topography modelling. *Nat. Hazards Earth Syst. Sci., 17*, 1837-1856

Khanal, N.R., Hu, J.-M., & Mool, P. (2015). Glacial lake outburst flood risk in the Poiqu/Bhote Koshi/Sun Koshi river basin in the Central Himalayas. *Mountain Research and Development, 35*, 351-364

Lee, E., Carrivick, J.L., Quincey, D.J., Cook, S.J., James, W.H., & Brown, L.E. (2021). Accelerated mass loss of Himalayan glaciers since the Little Ice Age. *Scientific reports, 11*, 24284

Popov, N. (1991). Assessment of glacial debris flow hazard in the north Tien-Shan. In, *Proceedings of the Soviet-China-Japan Symposium and field workshop on natural disasters* (pp. 384-391): USSR Shanghai, China

Rahman, M.M., & Bai, L. (2018). Probabilistic seismic hazard assessment of Nepal using multiple seismic source models. *Earth and Planetary Physics, 2*, 327-341

Sakai, A. (2012). Glacial lakes in the Himalayas: a review on formation and expansion processes. *Global Environmental Research, 16*, 23-30

Singh, A., Shrestha, D., Ghimire, K., Mishra, S., Rana, D., & Acharya, S. (2025). Assessing machine learning models to generate permafrost distribution map in Solukhumbu, Nepal. *Geodesy and Geodynamics, 16*, 275-287

Wang, X., Liu, S., Ding, Y., Guo, W., Jiang, Z., Lin, J., & Han, Y. (2012). An approach for estimating the breach probabilities of moraine-dammed lakes in the Chinese Himalayas using remote-sensing data. *Natural Hazards and Earth System Sciences, 12*, 3109-3122

Zhang, G., Bolch, T., Yao, T., Rounce, D.R., Chen, W., Veh, G., King, O., Allen, S.K., Wang, M., & Wang, W. (2023a). Underestimated mass loss from lake-terminating glaciers in the greater Himalaya. *Nature Geoscience*, 1-6

Zhang, T., Wang, W., & An, B. (2023b). A conceptual model for glacial lake bathymetric distribution. *The Cryosphere, 17*, 5137-5154